

Flexibility of Epichlorohydrin Production—Increasing Profitability by Demand Response for Electricity and Balancing Market

Journal Article**Author(s):**

[Lahrsen, Inga-Marie](#) ; Hofmann, Mathias; Müller, Robert

Publication date:

2022-04

Permanent link:

<https://doi.org/10.3929/ethz-b-000591770>

Rights / license:

[Creative Commons Attribution 4.0 International](#)

Originally published in:

Processes 10(4), <https://doi.org/10.3390/pr10040761>

Article

Flexibility of Epichlorohydrin Production—Increasing Profitability by Demand Response for Electricity and Balancing Market

Inga-Marie Lahrsen, Mathias Hofmann *  and Robert Müller 

Department of Energy Engineering and Environmental Protection, Technische Universität Berlin, Marchstraße 18, 10587 Berlin, Germany; inga.lahrsen@gmx.de (I.-M.L.); robert.mueller.2@tu-berlin.de (R.M.)

* Correspondence: hofmann@iet.tu-berlin.de; Tel.: +49-30-314-23229

Abstract: The increasing share of variable renewable energies in the power grid is an incentive to explore demand response strategies. Chlor-alkali processes are high potential candidates, according to previous publications. Within Germany’s chemical industry, chlorine production accounts for approximately 20% of electricity use and could play a significant role in power grid stabilisation on the consumer end. This study focuses on the feasibility of load flexibilisation in epichlorohydrin plants, with the second biggest estimated demand response potential for chlorine-based products in Germany. A plant model with allyl chloride storage was created based on real data and literature values. Results from this model, spot market and balancing power prices, and future electricity market scenarios were used in a mixed-integer linear optimisation. We find that benefits from demand response can be generated as soon as additional power and storage volume is provided. The composition of provided types of balancing power bids follows the price trend on the market. Additionally, the computation time could be lowered significantly by running the scenarios in parallel. The results encourage a practical validation of the flexibility of epichlorohydrin production.



Citation: Lahrsen, I.-M.; Hofmann, M.; Müller, R. Flexibility of Epichlorohydrin Production—Increasing Profitability by Demand Response for Electricity and Balancing Market. *Processes* **2022**, *10*, 761. <https://doi.org/10.3390/pr10040761>

Academic Editor: Matti Lehtonen

Received: 21 March 2022

Accepted: 10 April 2022

Published: 13 April 2022

Publisher’s Note: MDPI stays neutral with regard to jurisdictional claims in published maps and institutional affiliations.



Copyright: © 2022 by the authors. Licensee MDPI, Basel, Switzerland. This article is an open access article distributed under the terms and conditions of the Creative Commons Attribution (CC BY) license (<https://creativecommons.org/licenses/by/4.0/>).

Keywords: demand response; balancing power; chemical industry; epichlorohydrin process; optimisation; economic analysis

1. Introduction

Efforts to reduce CO₂ emissions have increased the use of variable renewable energy sources (VRE) worldwide, resulting in additional fluctuations in the power grid. In Germany, the share of renewable energies in gross electricity consumption is aimed for 65% by the year 2030 according to §1 (2) of the *Erneuerbare-Energien-Gesetz* (the Renewable Energy Sources Act), likely resulting in a more challenging grid operation management [1]. To contribute to the stabilisation of the power grid, demand response (DR) can be considered. For instance, a chemical plant is operated flexibly according to the currently available electricity on the market, see Figure 1. Additionally, frequency containment reserves (FCR), automatic frequency reservation reserves (aFRR) and manual frequency restoration reserves (mFRR) can be provided at balancing power (BP) market.

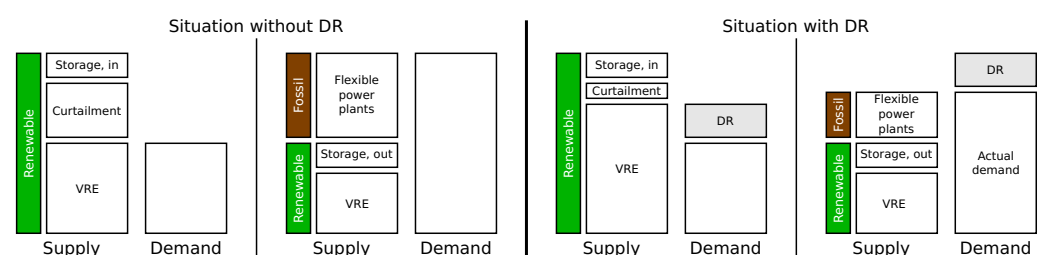


Figure 1. The equilibrium of supply and demand in future energy systems.

Following Torriti [2], we distinguish between DR and demand side management (DSM), which covers all activities to influence electricity consumption [3]. Figure 2 gives an overview of such activities, possible target groups, and time horizons. Demand response is defined by [4] as “changes in electric usage by end-use customers from their normal consumption patterns in response to changes in the price of electricity over time, or to incentive payments designed to induce lower electricity use at times of high wholesale market prices or when system reliability is jeopardised”. Two main types of DR can be described, cf. [2]. Based on pricing or reliability signals, customers are empowered to shift, to reduce, or to increase their load of electricity [5].

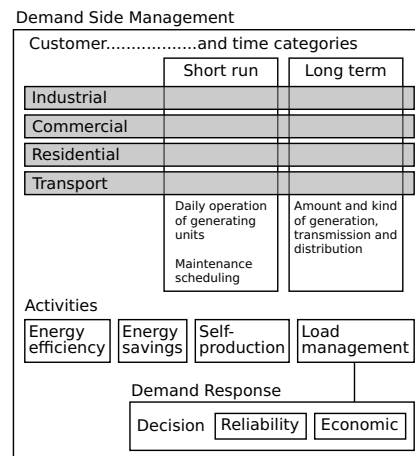


Figure 2. Demand side management categories: Demand response as an element; based on [3,5–7].

According to available publications [8,9], DR is beneficial for electrochemical industries to reduce their electricity purchase costs. Several electricity-intensive industries have already been studied for DR capacities, including the, considered suitable, chlor-alkali electrolysis (CAE) process, which accounts for approximately 20% of the German chemical industry’s electricity consumption [10] with a total installed power of 1350 MW [11]. This considerably high consumption justifies the investigation of CAE based plants’ DR potentials as an option in grid stabilisation relevant. Further, Arnold et al. [12] mentioned that the conflict between efficiency and flexibility is an essential hurdle from the industrial point of view. Since the efficiency of electrolysis increases at part load [13], the investigation of DR potentials at CAE plants gains even more importance.

Demand response requires the presence of a storage tank if load shifting is applied [13]. Chlorine or subsequent products are stored in case of overproduction to guarantee a constant final product feed throughout a fixed time horizon. In previous publications, several CAE models with chlorine storage were implemented and investigated for DR [14–18]. Otashu et al. [14] focus on the membrane cell and cell energy modulation restriction and find that the CAE process allows for short-term changes in power consumption. Wang et al. [15] embed the CAE process into a hybrid renewable energy system which includes operating and environmental costs and receding horizon optimisation. They find that production costs can be significantly reduced and profits increased. Chen et al. [16] also model a hybrid system with a CAE plant that produces hydrogen for a fuel cell. Their research focus is on the operation and control of the system. Baetens et al. [17] propose a deterministic co-optimisation model of electricity sourcing and FCR delivery with short term price prediction. Optimisation models with price forecasting, assumption of future price knowledge and flat load are investigated for cost benefits from flexibility. Their results show that a flexible operation of CAE is of interest when the day-ahead market prices present high fluctuation. Teichgraeber et al. [18] apply a stochastic optimisation model to study the effect of price uncertainty on plant design decisions with the result that flexibilisation of plants with oversized components can enhance participation in electricity markets and increase profits. Overall, these previous research contributions show that, with chlorine

storage, the flexibilisation of CAE plants with interaction at the energy spot market or the balancing power market, variable costs can be reduced.

However, industrial chlorine is primarily stored in quantities of a couple of hours of production to two days for safety reasons [10]. Besides a model of Richstein et al. [19] that represents not only the CAE process, but also the further production of ethylene dichloride (EDC), limited research of DR potentials of chemical processes based on CAE is available. Klauke et al. [20] evaluate the detailed research of DR potentials of chlorine-based chemical production processes. Apart from the DR potential of the polyvinyl production via the EDC route, being the main consumer of chlorine in the chemical industry in Germany [20] and which was afterwards studied by Hofmann et al. [21] for the German energy market, the epichlorohydrin (ECH) production was suggested to be the second promising candidate for DR. It is characterised by a considerably high chlorine consumption and a flexibility potential of 26 MW as well as the highest specific electrical energy demand per mass unit of product based on the available positive DR [20].

Moreover, previous research of DR potentials is mainly limited to electricity markets. Either historical electricity prices or stochastically modelled prices [18] are used to feed the optimisation models. Hofmann et al. [21] and Richstein et al. [19] provide outlooks on DR potentials based on spot prices from future electricity market scenarios. However, the future of electricity markets will likely be influenced by a more significant share of renewable energies or rising carbon dioxide prices. Therefore, in this study, it was of interest to link the plant model for DR potential research to future electricity market scenarios. Besides, only a few publications include DR potentials from balancing power markets such as FCR [17] and interruptible loads [19]. Furthermore, Richstein et al. [ibid.] find that day-ahead flexibility and reserves from FCR and interruptible loads are substitutes for each other and that the participation in the balancing power market can even restrict the participation in other markets. Nevertheless, changes in balancing power supply regulations in terms of shorter time blocks and the possibility of pooling in Germany provide new incentives to research the economic benefits of DR not only on the spot price market but equally regarding balancing power price fluctuation and regulatory changes since 2017. This article focuses on the economic benefits of the DR potential of the industrial ECH process as a whole, a consideration of all types of balancing power on the German market and the optimisation of the computational modelling.

Besides this, computation time minimisation is examined in other articles and explicitly addressed by some of the above mentioned authors. Otashu et al. [14] reach a computation time of 3 days with 30 iterations without improvement for a model with 1780 equations of which 30 are differential. Baetens et al. [17] use a Hammerstein-Wiener modelling approach to decrease the computational time. Teichgraeber et al. [18] apply scenario reduction techniques to investigate if computation time decreases for their stochastic optimisation formulation. They find that scenario reduction leads to satisfactory objective function value estimation, while errors in design decision occur. In all these articles computation time reduction is approached by adaption of the models themselves. In this study, the improvement of computation time is achieved by parallelisation of scenario runs on several kernels and not within the model.

Furthermore, Ausfelder et al. [22] differentiate between theoretical and technical flexibility: the difference between full load and actual load, in theory, should be analysed regarding operating conditions to estimate a plant's DR potential. Bruns et al. [23] define detailed categories of flexibility for the chemical industry. They argue that the concept of flexibility in this field lacks comprehensive organisation. According to their definition, the modelled plant in this study covers the apparatus and process level and neglects the process environment.

The aim of this work is to provide an ECH-plant model with flexible allyl chloride (AC) production to investigate the DR potential in terms of economic viability in both spot and balancing markets. All calculations are carried out using real plant data or specifications from the literature. All input data, simulations, optimisations, and results can

be obtained via zenodo [24]. The novelty of this article is the investigation of flexibility of ECH production, as a subsequent chlorine based product. The optimisation model includes prices of all types of balancing power and future electricity market scenarios [25,26].

The article is structured as follows: The ECH production process, the models, and the methodologies applied here are summarised in the next section. The results of the investigation are presented and discussed in Section 3, which is followed by the conclusions.

2. Methodology

In Section 2.1, a detailed description of the ECH plant is given, and important flexibility parameters are discussed. On this basis, a plant model was developed using Engineering Equation Solver (EES) [27], see Section 2.2. The resulting correlations of product stream and power from the electricity grid for different maximum power of the plant are used for the optimisation problem, which was developed using General Algebraic Modelling System (GAMS) [28] and solved using CPLEX [29], see Section 2.3. GAMS is a proprietary software framework for mathematical optimisation, its syntax is designed as an algebraic modeling language. In the context of optimisation in GAMS, a sensitivity analysis for the parameters maximum power, bid rate and AC storage volume is presented. For the purpose of run time reduction, the call of different optimisation scenarios was paralleled, presented in Section 2.4. All input data, simulations, optimisations, and results can be obtained via zenodo [24].

2.1. Plant Model

A literature review of industrial CAE and ECH processes was conducted to develop the simulation model of the plant in EES. Three industrial plant locations in Germany produce ECH in a quantity of at least 150 kt per year according to a market analysis from 2018 [30]. Based on the propene route, ECH can be obtained via four chemical reactions, which are considered in the model. A flowchart of the overall process is presented in Figure 3. It is used as an intermediate product for further synthesis in the epoxy resin, glycerine, drug and paper industry [31]. The process parameter conditions of the CAE unit were settled in dialogue with industrial plant operators.

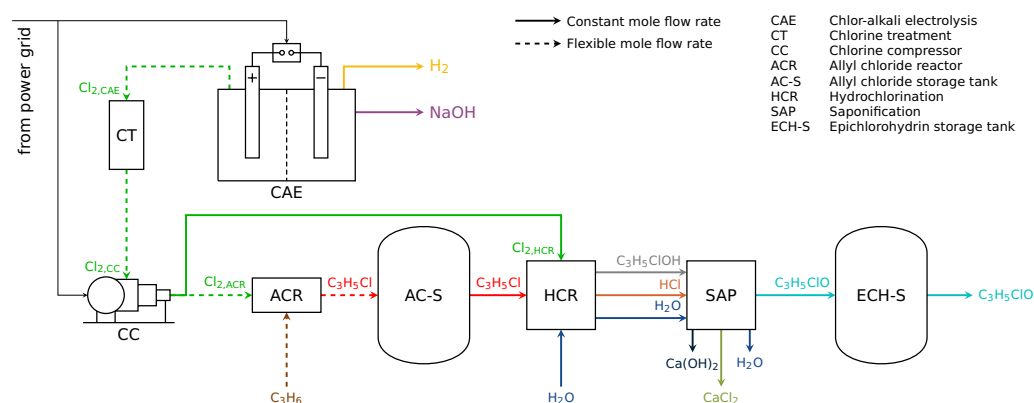


Figure 3. Flowchart of the ECH production process.

2.1.1. Chlor-Alkali Electrolysis

Chlorine is produced in the CAE process, see Equation (1). Ausfelder et al. [22] have assessed a flexible CAE operation with membrane cell type, being the most common design in Germany [32], as feasible. According to Arnold et al. [12], it is the most suitable CAE technology for DR. To ensure high purity, chlorine is liquefied under compression [33,34]. It is assumed that an isentropic turbo compressor with six stages for large quantities is sufficient [33] to compress the chlorine to 1.2 MPa at 30 °C to fulfil regulations for overground compressed gas-tanks that have to be protected against heat [35]. The liquid chlorine is decompressed before further reaction. The compressor unit design ensures temperatures be-

low 100 °C [36] after each compressor stage to inhibit ignition of equipment [33]. The CAE unit has a reference power of 100 MW resulting in an ECH production rate of 135 kt per year, which is within the scale of the German industry. A share of 3.33% of the chlorine is fed back to the CAE unit for acidification of the electrolytes. Based on the EES model, a constant mole flow rate of 65 mol/s was calculated as feed to the hydrochlorination reactor (HCR) to ensure a constant ECH production as under reference condition. It was assumed that the produced hydrogen and caustic soda could safely be stored as regularly done in the industry.



2.1.2. Allyl Chloride Reactor

Gaseous chlorine at ambient temperature and propene at 400 °C are converted into allyl chloride in an exothermic reaction ($\Delta H_R = -113 \text{ kJ/kg}$, molar ratio 1:5) in a tube reactor, see Equation (2). The conversion rate of chlorine is assumed to be 86% [37]. A sensitivity analysis was carried out with a stationary integral heat balance of the AC reactor to estimate the effect of variable propene temperature, chlorine feed rate and molar ratio on the reactor temperature. The mass fractions of the reactands were logarithmically averaged to calculate the mean heat capacity of the gas mixture. The propene temperature was found to be the parameter with the strongest influence. It was assumed that it could be controlled together with the feed rate to ensure a constant molar feed ratio in the preheating stage. An AC storage tank is installed after the reactor, assuming that AC, with a considerable higher dew point, can be separated from other components in the outlet stream by condensation.

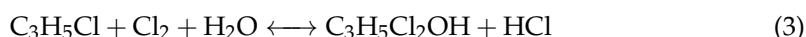
The flexibilisation of the saponification step with an ECH storage was considered for the installation of a storage unit because it was classified as rather resistant to disturbances by industrial plant operators. Still, this would imply controlling all process parameters such as temperatures and feed ratios under the flexibilisation of the preliminary process steps. Concerning the sensitivity analysis of the AC reactor temperature and to simplify the control of the process under load shifts, the installation of an AC storage unit was found to be most suitable.

The arrangement of the storage tank (AC-S) downstream of the reactor (ACR) prevents interferences in the following AC purification steps by separation columns which are neglected henceforth. Furthermore, the additional effort in the complexity of control engineering is moderate. The storage of other products in the following process chain was excluded because of product instability and the sensibility of process steps.



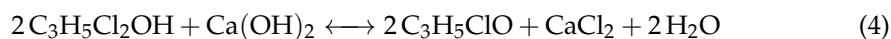
2.1.3. Hydrochlorination

For hydrochlorination, Equation (3), AC is fed to a continuous stirred tank reactor with water to AC volume ratio of 50:1. Chlorine is fed with a molar ratio of 1:1 based on AC. The conversion rate of AC is assumed to be 92% [38,39].



2.1.4. Saponification

Ultimately, ECH is obtained in the chemical reaction of $\text{C}_3\text{H}_5\text{Cl}_2\text{OH}$ (conversion rate: 94%, molar ratio $\text{Ca}(\text{OH})_2:\text{C}_3\text{H}_5\text{Cl}_2\text{OH}$ of 1:1.5 [40]) and calcium hydroxide in an aqueous solution in Equation (4). It is assumed that HCl is removed after the saponification step.



2.2. Model Equations and Parameters in EES

The model starts with the design of the CAE Equation (1). Faraday's law of electrolysis was used to describe the electrochemical redox reaction, see Equation (5). It is applied

with an efficiency of 96%, 1440 stacks and a factor for additional power, which is based on information from the chlorine industry [21].

$$\dot{n}_{\text{Cl}_2, \text{CAE}} = \frac{I}{2 \cdot 96.485 \text{ kA s/mol}} \cdot \frac{\eta_{\text{CAE}}}{100} \cdot N_{\text{stacks}} \cdot (1 + k_{\text{add}}) \quad (5)$$

The cell voltage was calculated from Equation (6).

$$U = \frac{I}{A_m} \cdot 0.142 \text{ V m}^2/\text{kA} + 2.423 \text{ V} \quad (6)$$

From the produced chlorine, a constant mole flow rate is needed for the hydrochlorination, see Equation (7). The remaining chlorine is used for AC production.

$$\dot{n}_{\text{Cl}_2, \text{ACR}} = \dot{n}_{\text{Cl}_2, \text{CAE}} - \dot{n}_{\text{Cl}_2, \text{HCR}} \quad (7)$$

Mass balances were carried out with the previously described efficiencies for each step to link the Faraday equation to the AC production, the storage tank's inlet stream. A steady-state process is assumed, and the thermodynamic properties are calculated with the ideal gas law. Heat losses and additional power demand except CAE and chlorine compression are neglected to simplify the modelling.

The power from the grid is used for the electrolysis and the turbo compressor, Equation (8). The reference power includes a loss from the transformer of 3.43%. The compressor power consumption is modelled with six stages, as mentioned above.

$$\dot{W}_{\text{grid}} \cdot \frac{\eta_{\text{transform}}}{100} = \dot{W}_{\text{comp}} + \dot{W}_{\text{CAE}} = \dot{W}_{\text{ref}} \quad (8)$$

2.3. Optimisation and Sensitivity Analysis in GAMS

The total power of the modelled CAE plant was extended by 5%, 10%, 20% up to 40% based on the reference power according to Equation (9).

$$\dot{W}_{\text{total}} = \dot{W}_{\text{ref}} \cdot (1 + k_{\text{add}}) \quad (9)$$

The electrolysis efficiency of a CAE cell increases at part load [21]. This results in a reduction of the minimum power supply to maintain the ECH production at reference state and thus in increased DR flexibility, as shown in Figure 4 when power in terms of extra cell stacks is added. The minimum required power to ensure chlorine production for hydrochlorination, when allyl chloride is taken from storage, decreases for the same reason but with a lower gradient since the relation of chlorine production and power is described by a concave curve. Figure 4 represents the result from the plant model. For optimisation purposes the nonlinear function for the correlation between mole AC stream and total power

$$\dot{n}_{\text{AC}}(t) = f(\dot{W}_{\text{total}}(t)) \quad (10)$$

was piecewise linearised. Introduced binary variables ensure that only one linear function is active at every time step, such as performed by Bree et al. [41]. It was considered that CAE operation below 4.2 A/m^2 current density (used as a lower bound in an industrial plant) of the maximum load can have a significant impact on the product quality of caustic soda. Therefore, both a fixed lower bound of 4.2 A/m^2 as well as the lower bounds resulting from production rate requirements were considered.

The objective cost function Equation (11) for flexible operation through DR consists of expenses for power from the grid for CAE, additional expenses for material wear out, and returns from balancing power supply. Costs for wear out of CAE cell components such as the membrane were estimated in a previous study [21]. Therefore, simulations with costs of 5000 € per full load cycle were performed as well as simulations that neglect such costs. The total costs are minimised at every hour throughout the year with a solver

for mixed-integer linear problems (MIP). The relative tolerance was set to 0.001 based on the optimal solution for the objective function in order to meet a reasonable computation time. Electricity prices in hourly resolution are provided as input for the model. Hence a perfect price forecast was assumed. The time slices for balancing power supply correspond to the regulations in Germany, which were reformed for aFRR in 2018 and FCR in 2019. Before July 2018, time slices for aFRR are divided into main time on weekdays between 8 a.m. and 8 p.m. and remaining time, subsequently in six 4 h-blocks. FCR is provided in weekly time slices before July 2019 and then in 24 h-blocks. Meanwhile, mFRR is provided in six 4 h-blocks in every simulation. The model assumes that power shifts occur instantly.

$$OBJ = \min \left(\sum_t c_E \cdot \dot{W}_{\text{grid}}(t) \cdot \Delta t + \sum_t C_R(t) - \sum_t C_{BP}(t) \right) \quad (11)$$

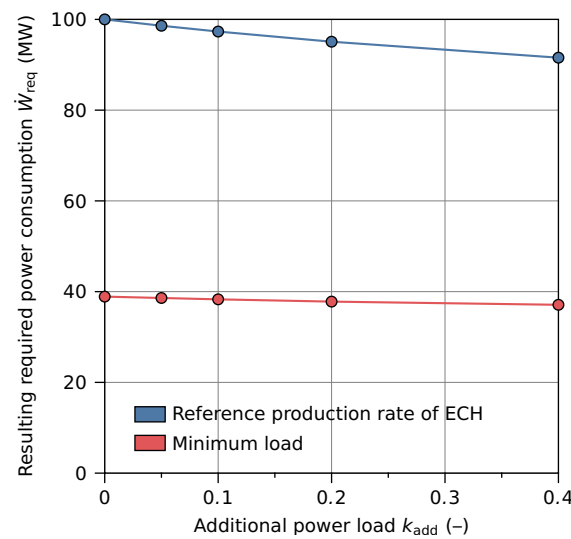


Figure 4. Minimum load and power consumption at reference production rate of ECH according to additionally installed power.

In the optimisation model, the maximum offer of DR volume is calculated on the basis of AC storage level. A mass balance is carried out to determine the amount of stored AC that can be used as a buffer to produce ECH while offering positive balancing power. The remaining volume in the storage tank can be used to offer negative balancing power. In the model, only the provision of balancing power is covered. The amount of balancing energy that is effectively accessed is not verified.

In terms of sensitivity analysis, additional power, AC storage volume and the maximum bid factor for FCR, aFRR and mFRR has been varied, one variable per scenario, see Table 1. The reference amount of balancing power was set to 1% for FCR, 5% for aFRR and 10% per time step for mFRR based on the total power of the CAE plant and varied, Equation (12).

$$b = b_{\text{max}} \cdot b_{\text{ref}} \quad (12)$$

The bid rates for each type of BP were set arbitrarily, according to the allowed duration of load change and latency [13]. Thus, for FCR with the lowest load change duration and latency, less balancing power is allowed than for aFRR and mFRR in order to save time for the chemical plant to adapt to the load change. Load ramp velocities as well as other possible factors influencing the maximum offer of DR volume should be investigated further. The additional storage volume is calculated as shown in Equation (13), where the reference volume V_{ref} of 19 m³ represents the production of ECH within one hour at reference load.

$$s = s_{\text{add}} \cdot V_{\text{ref}} \quad (13)$$

Table 1. Parameters of sensitivity analysis.

Parameter	Symbol	Unit	Value
Additional power	k_{add}	-	0, 0.05, 0.1, 0.2, 0.4
Additional storage volume	s_{add}	-	0, 1, 2, 4, 8, 16, 32, 64, 128
Maximum bid factor ^a	b_{max}	-	0, 1, 2, 4, 6

^a Factor refers to reference bid size b_{ref} : FCR 1%, aFRR 5%, mFRR 10%.

The optimisation results in GAMS with lower load boundaries based on the EES model were compared to results with a fixed lower bound based on information of operation limits from the industry: It was considered that CAE operation below 52% (corresponding to 4.2 A/m² used as a lower bound in an industrial plant) of the maximum load can have a significant impact on the product quality of caustic soda.

Historical spot and balancing power prices in Germany from 2017, 2018 and 2019 were used to investigate the benefits of the ECH production as an actor on the balancing market. Additionally, two spot price fundamental models, the model from Koppeske et al. [26] and EMMA model [25], were applied to forecast future DR potentials concerning spot price volatility. Balancing power services are not part of the simulation of future DR potentials.

1. The model called Electricity Market Model (EMMA) for 2025 and 2030, which takes into account the goals of the German government to increase the share of renewable energies in the gross energy consumption to 40–45% by 2030 [42], prices carbon dioxide at 57 €/t and gives spot prices in hourly resolution [43]. In the model, the share of renewable energies in the grid has an impact on the price level—more renewables decrease the electricity price in the model for the reference year 2016. The assumption that the energy demand can be covered from the supply side at all times reduces the overall price volatility. Still, scarcity prices can occur in order to cover the supply. The modelled average hourly spot price for 2025 is 50 €/MWh with a standard deviation of 37 €/MWh and for 2030 53 €/MWh with a standard deviation of 53 €/MWh.
2. The model of Koppeske et al. for the year 2035, which estimates prices based on higher shares of lignite and hard coal (20 GW) and a lower share of renewables (190 GW) than aimed by the German government by that year. The average hourly spot price for 2035 is 63 €/MWh with a standard deviation of 36 €/MWh.

2.4. Parallelisation

Calling all 225 scenarios in nested loops within one single GAMS run, RAM limitations of the server may force abortion of the calculation. The run-time per scenario increases with added storage volume for each performed power below 120 MW. The bottleneck arises with power capacities of 120 MW and above in addition to small storage capacities. Therefore, Algorithms 1 and 2 were used, which calls each scenario and pipes it to an individual GAMS run, using the GNU command *parallel*.

Algorithm 1: routine to run all scenarios in parallel mode

Data: list (csv-file) with values for each parameter of sensitivity analysis, see Table 1

Result: one directory for each scenario including GAMS program and list in inc file format with scenario-dependent parameter settings

```

1  initialisation of  $h, i, j, k_{add}, s_{add}, b_{max}$ ;
2  make directories scenarios and results;
3  introduce  $a = ()$ ;
4  for  $h \leftarrow 1$  to count of values of  $k_{add}$  do
5      copy  $h^{th}$  value from list of  $k_{add}$  to respective GAMS parameter;
6      print GAMS parameter to inc file;
7      for  $i \leftarrow 1$  to count of values of  $s_{add}$  do
8          copy  $i^{th}$  value from list of  $s_{add}$  to respective GAMS parameter;
9          print GAMS parameter to inc file;
10         for  $j \leftarrow 1$  to count of values of  $b_{max}$  do
11             copy  $j^{th}$  value from list of  $b_{max}$  to respective GAMS parameter;
12             print GAMS parameter to inc file;
13             append composed value of  $hij$  to  $a$ ;
14             make directory named  $hij$  inside of directory scenarios;
15             copy generated inc files to directory  $hij$ ;
16             copy GAMS code to directory  $hij$ ;
17         end
18     end
19 end
20 use GNU command parallel to distribute shell script calls of Algorithm 2 with 1 :::
    a[*] as transferred parameter in terms of threads to all kernels ;

```

Algorithm 2: GAMS call for each scenario

Data: Transferred parameter a from Algorithm 1

Result: calls GAMS code within each directory created in Algorithm 1

- 1 Open directory with name corresponding to value of a ;
- 2 Run GAMS script with parameters stored in the inc file in the corresponding directory created in Algorithm 1;

3. Results

In the following, the results for computation time and economic benefits from DR are presented separately. The computation time behaviour is presented to show potential of reduction when the optimisation problem is run in parallel. Moreover, results for economic benefits from DR within the sensitivity analysis influenced by varying additional power, storage volume and bid factors for BP are discussed. This discussion is based on the benefits from the day-ahead and balancing power market in the past and modelled day-ahead market prices for future scenarios.

3.1. Computation Time

Figure 5 shows computation times of all scenarios, which depend mainly on the installed additional CAE power and storage volume. For capacities of 100 MW, 105 MW and 110 MW, it increases with the storage volume as well as bid factor for balancing power. At 120 MW and 140 MW, the bottleneck arises at small storage volumes combined with an allowance for balancing power provision. The maximum computing time increases from around 17 min to 228 min. With increasing storage volume, the computing time decreases to values in the range of scenarios below 120 MW. Hence, the storage volume appears to be a limiting factor and a variety of solutions, including balancing power provision, might be suitable. The parallelisation (12 threads) of the scenario calls reduces the overall

computation time from four days to around five hours. In case of sequential calculation using a single GAMS call on one CPU, the server runs short on RAM capacity and is not able to finish the calculation for all scenarios. For the year 2018, the computation time for scenarios with high additionally installed power (20 MW) and small storage volume is up to a factor of approximately 20. Here, a correlation with the regulatory changes for balancing power towards more flexibility is probable. Before July 2018, blocks for aFRR and mFRR were tendered weekly and then changed to daily tendering. For FCR the same adaption was undertaken in July 2019. The provided BP blocks are activated when switching binary variables as prefactors to one. A reduction of hours per BP block reduces the number of linked binary variables. When these smaller BP blocks of different sizes are combined, this reduces the overall computation time, compared to the case with larger BP blocks.

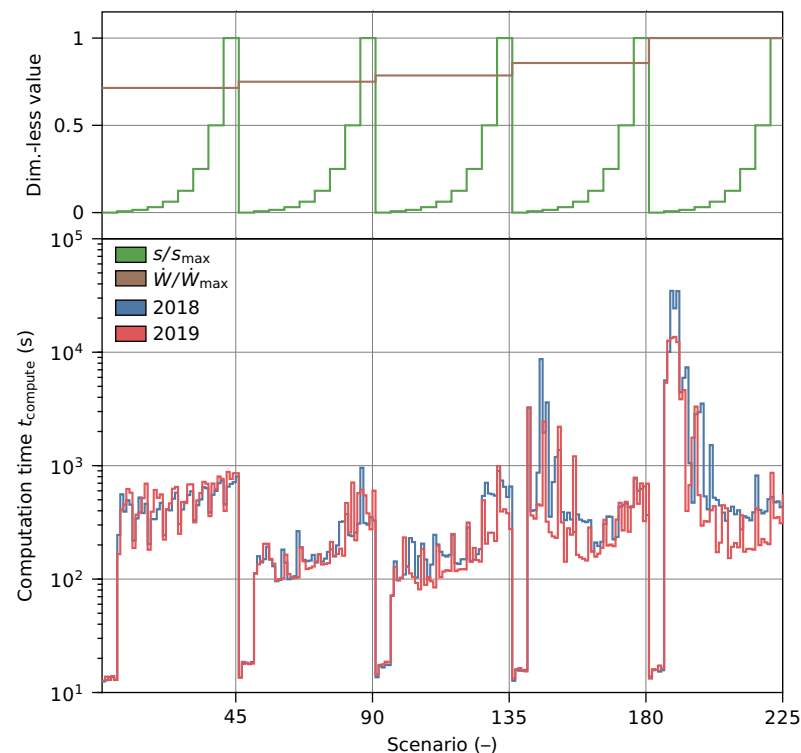


Figure 5. Computation time over increasing total power \dot{W}_{total} , storage volume s and bid factor b_{ref} .

3.2. Economic Benefits

To start with, an adjustment in the model of the lower load bound barely reduces the savings: with consideration of BP the difference is below 5% and with consideration of spot price market only below 1% since no BP potential from additional load reduction is taken into account. Further, even though, the cost of membrane and electrode wear-out could not be determined and was therefore modelled as a variable, results show that different cost scenarios between zero and 5000 € per load cycle show insignificant deviations (4.8% with and 0.6% without balancing power) and maximum AC storage capacity in terms of overall cost savings.

In order to benefit from cost reduction for grid utilisation, the plant has to be operated at least 7000 h at full power load per year, which limits the installed power to 120 MW. The investment of 20 MW allows for savings of 1.63×10^6 € due to part-load efficiency increase of the CAE and total savings of 3.7×10^6 € with a storage volume of 32 h of reference production (based on 2019, no costs for material wear-out). For the simulation results, DR savings increase with a logarithmic trend; hence a storage volume of 32 h of reference production represents 2.07×10^6 € of savings. The additional supply of balancing power at maximum bid factor (6% FCR, 30% aFRR, 60% mFRR) results in total savings of 3.25×10^6 € at 32 h storage. It further shows that it is beneficial to supply balancing power

when a storage unit is installed. With an AC storage capacity of 152 m^3 , the difference in savings of an ECH plant with a maximum power 105 MW and maximum bid factor compared to a maximum power of 140 MW without balancing power is $0.34 \times 10^6 \text{ €}$.

Figure 6 shows the reduction of electricity purchase costs for the years 2017, 2018 and 2019. Without storage capacity, the additionally installed power of 20 MW results in cost savings of $1.48 \times 10^6 \text{ €}$ for 2017, $2 \times 10^6 \text{ €}$ for 2018 and $1.63 \times 10^6 \text{ €}$ for 2019 from increased CAE efficiency at part load. The savings increase up to $3.69 \times 10^6 \text{ €}$ (2017), $4.12 \times 10^6 \text{ €}$ (2018) and $3.41 \times 10^6 \text{ €}$ (2019) with a storage volume of 32 h of nominal operation of 19 m^3 ECH production per hour at reference load. Table 2 lists the average yearly price levels and price spreads, which affect the cost savings, when storage capacity of AC is offered. The cost savings for 2017 exceed 2019 at capacities of 16 h and more with a higher average spot price in 2017 than 2019, but higher price spread in 2017 than 2019.

Table 2. Mean yearly price levels given in €/MWh on the spot market including standard deviation σ , database [44].

Year	2017		2018		2019	
	Average	σ	Average	σ	Average	σ
	34.19	17.66	41.73	16.61	37.67	15.52

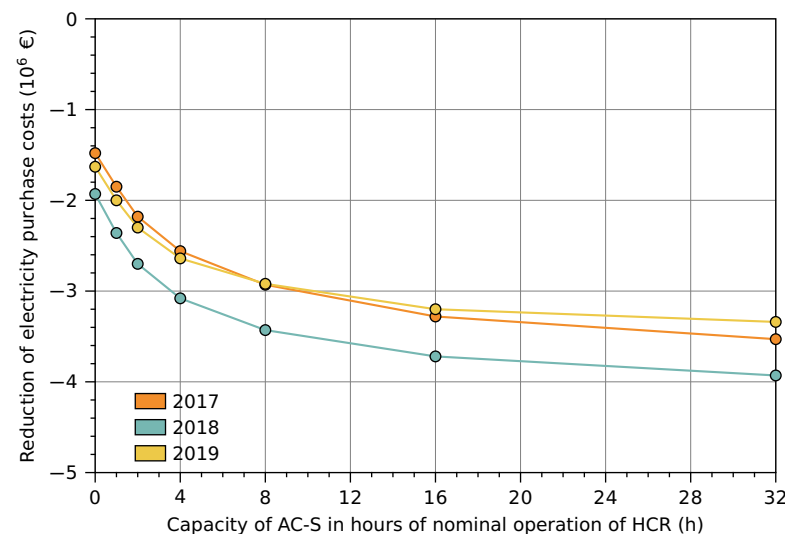


Figure 6. DR savings without balancing power service, 120 MW, 2017–2019.

Spot prices from the EMMA model present comparably low volatility with a price spread of 3 €/MWh compared to the historic spot price spread of 12 €/MWh in 2016 [21], thus offering less economic incentive for DR, which could be shown by simulating DR operation with historical and modelled (EMMA) spot prices from 2016. For future predictions in Figure 7, the difference in cost savings based on DR is more significant than on part-load efficiency (2025: $2.17 \times 10^6 \text{ €}$, 2030: $2.31 \times 10^6 \text{ €}$, 2035: $2.69 \times 10^6 \text{ €}$): with additional storage of 32 h and DR with maximum bid factor, savings can be augmented to $3.38 \times 10^6 \text{ €}$ in 2025, $4.72 \times 10^6 \text{ €}$ in 2030 and $7.61 \times 10^6 \text{ €}$ in 2035.

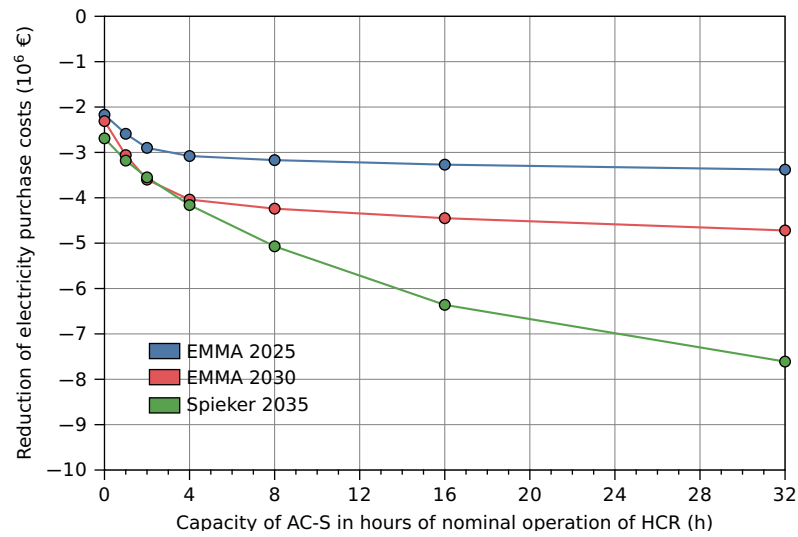


Figure 7. DR savings without balancing power service, 120 MW, 2025, 2030, 2035 based on modelled spot prices.

Figure 8 illustrates simulated income from the balancing market for a storage of 32 h, split into the respective types FCR, positive aFRR, and mFRR, as well as negative aFRR and mFRR. The results show that the allowed volumes are exploited depending on the simulated year. In 2017, proceeds of 9.32×10^6 € were close to double as high as in 2018 and 2019. The dominating parts of balancing power types vary from positive aFRR in 2017 and 2018 to positive mFRR in 2019. Proportionally, the types of balancing power remain stable with increasing bid factor every year. The allowed volume for provision per type arising from the maximum bid factor b_{max} does not mirror the distribution of income as e.g., aFRR and FCR outweigh mFRR, with the highest allowance, in 2017 and 2018. Overall income from balancing power increases with the bid factor in the same way proportion-wise for every single year. It was observed that the provided variable amount of storage volume was no limiting factor for the provision of BP in the optimisation model regarding the allowed BP volume. Concerning the yearly average prices per balancing power type in Table 3, one important driving factor for balancing power provision and income proportion is the price level, as prices correlate with the optimised amount of provided balancing power.

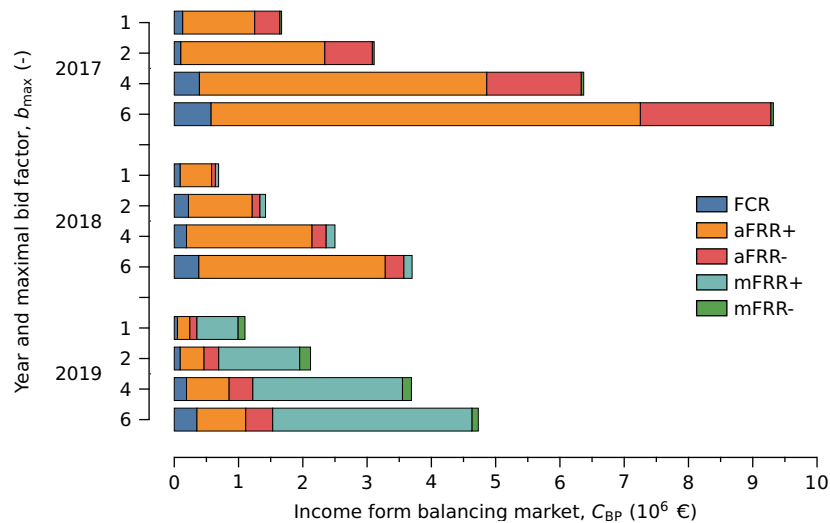


Figure 8. Incomes from balancing market, 32 h storage, 120 MW.

Table 3. Mean yearly price levels given in €/MWh on the balancing market including standard deviation σ , database [45].

Year	2017		2018		2019	
	Average	σ	Average	σ	Average	σ
FCR	14.61	2.44	12.66	3.14	8.84	2.47
aFRR+	23.25	19.75	10.69	11.55	3.76	6.84
aFRR−	21.57	21.00	1.89	5.30	3.62	4.75
mFRR+	0.06	0.65	4.18	6.98	6.14	36.95
mFRR−	0.70	2.62	0.94	3.27	2.32	4.88

4. Conclusions

Regarding technical feasibility, both AC synthesis and saponification of dichlorohydrin were considered for flexibilisation. AC synthesis was chosen to reduce potential control and instrumentation costs since fewer product streams and process parameters have to be controlled with respect to the modelled energy and mass balances. The flexibilisation requires a constant chlor-propene-ratio and a stable preheating temperature of propene. The modelled minimum load of the CAE ensures a stable ECH production; caustic soda quality related to CAE load reduction was not considered in this research. Moreover, it was found that the load shifts rarely meet the lower bounds since the economic benefits do not vary significantly.

In terms of cost of membrane and electrode wear-out, results show that different cost scenarios between zero and 5000 € per load cycle show insignificant deviations in terms of overall cost savings. In the model, flexible AC production combined with the provision of balancing power is a profitable alternative to the sole flexible power purchase, when a storage unit is installed. At the additional power of 5 MW, a balancing power bid factor of 6 and a storage volume of 152 m³, more benefit is generated than with demand response for flexible power purchase only at additional power of 40 MW.

For the balancing power market, the results show that economic benefits regarding bid shares correlate to the corresponding mean price levels per year, which show no stable trends between 2017 to 2019. However, it must be further investigated if changes on the balancing power market towards bids for shorter time slices for PRL in 2019 and SRL in 2018 lead to increased offered provision of these BP types. Despite the predicted savings in the optimisation results, for industrial plant management, it will be challenging to decide on a product type constitution without the absolute price forecast given to the model. Still, it needs further investigation to estimate CAE plants' realistic technical bid rate for balancing power supply.

The analysis of future DR opportunities concludes that economic benefit is generated with electricity prices from both the Kopsiske et al. model and the EMMA model. Suppose the effect of lower price volatility of the EMMA model compared to actual spot prices from the past applies in the future. In that case, actual cost savings from DR could turn out higher than predicted by the optimisation model. Although price volatility was found to be reduced, scarcity prices possibly provide an incentive for DR since cost savings are within and above the range from 2017 to 2019. For the Kopsiske et al. model, price volatility appears to be comparable to 2017 to 2019, which, together with higher spot prices, leads to increased cost savings.

The savings from DR and provision on the balancing market have to be contrasted with arising expenses for the storage unit, investment in CAE power, and membrane material wear-out. According to the simulation results, savings from DR primarily depend on the volatility of the spot market prices and the balancing power market price level.

In relation with previous studies, the comparison of flexibilisation of plant models based on CAE and the effects on the electricity costs are of interest. Regarding the results from Hofmann et al. [21] and Richstein et al. [19], the benefits from DR in this study follow the quantitative trend, meaning that DR benefits increase with AC storage capacity. For the

year 2018 Hofmann et al. modelled a CAE based ethylene dichloride plant with a nominal power load of 100 MW and found that cost savings could increase to approximately 4×10^6 € with an equivalent product storage of 16 h, a minimum power load of 30 MW and additional power of 20 MW. Compared to the results in this study, the savings of Hofmann et al. are marginally higher, which could stem from a greater flexibility range. Richstein et al. modelled a CAE plant for ethylene dichloride production with a reference power of 80 MW. An additional power of 40 MW and a maximum storage volume of 1000 t of ethylene dichloride resulted in a reduction of wholesale electricity costs to around 80% of the reference costs, accounting for specific costs of approximately 6 €/MWh. For comparison, projected over a year with 8760 h of operation, the cost savings represent around 6×10^6 € for the year 2015. Again, the minimum power load of 20 MW is lower than in this study and the results display greater cost savings. Overall, the cost savings from this study reflect the magnitude of previously published cost savings from flexibilisation. However, it has to be considered that both Hofmann et al. and Richstein et al. include fix costs in the models, which is not investigated in this study. Nevertheless, installing a storage and additional power creates benefits in any run scenario.

Finally, future research contributions will cover ramping and bidding limitations in their optimisation models. From this perspective, it has to be considered that the resulting cost savings from the model represent a best-case scenario. In any case, the absolute benefits of DR for ECH plants have to be put into context with operation and plant design costs. The sensitivity analysis in this study is the basis for a validation as it was done by Hoffmann et al. [13] based on the model of Hofmann et al. [21] for flexible PVC production. In a next step, the results should be validated by putting design decisions from the model to practice.

Author Contributions: Conceptualisation, I.-M.L. and M.H.; methodology, I.-M.L. and M.H.; software, I.-M.L.; validation, I.-M.L., M.H. and R.M.; formal analysis, I.-M.L.; investigation, I.-M.L.; resources, M.H. and R.M.; data curation, I.-M.L.; writing—original draft preparation, I.-M.L.; writing—review and editing, M.H. and R.M.; visualisation, M.H.; supervision, M.H. and R.M.; project administration, M.H. and R.M. All authors have read and agreed to the published version of the manuscript.

Funding: The authors gratefully acknowledge the financial support of the German Federal Ministry of Economic Affairs and Energy for the project ChemEFlex (project number 0350013A).

Data Availability Statement: All models and data used for the analysis of the flexible and economical operation of chlor-alkali process with subsequent epichlorohydrin production are available, see [24].

Conflicts of Interest: The authors declare no conflict of interest.

Nomenclature

Abbreviations

AC	Allyl chloride
ACR	Allyl chloride reactor
aFRR	Automatic frequency restoration reserves
BP	Balancing power
CAE	Chlor-alkali electrolysis
CC	Chlorine compressor
CT	Chlorine treatment
DR	Demand response
DSM	Demand side management
E	Electricity
ECH	Epichlorohydrin
EDC	Ethylene dichloride
EEG	Erneuerbare-Energien-Gesetz (Renewable Energy Sources Act)
EES	Engineering Equation Solver
EMMA	European Electricity Market Model

FCR	Frequency containment reserves
HCR	Hydrochlorination reactor
mFRR	Manual frequency restoration reserves
MIP	Mixed integer linear problem
R	Ramping
RAM	Random access memory
S	Storage tank
SAP	Saponification
VRE	Variable renewable energy sources
<i>Latin symbols</i>	
a	Array, –
A	Area, m ²
b	bid factor, –
c	Specific costs, €/MWh
C	Total costs, €
h	Incrementer
H	Enthalpy, J/kg
I	Current, A
i	Incrementer
j	Incrementer
k	Additional power based on reference power, –
\dot{n}	Mole flow rate, mol/s
N	Number, –
OBJ	Objective function, €/a
s	Storage volume, m ³
t	time, hour
U	Voltage, V
V	Volume, m ³
\dot{W}	Power, MW
Y	Binary variable, 0 or 1
<i>Greek symbols</i>	
Δt	Fixed time step width, 1 h
η	Energetic efficiency, –
σ	Standard deviation, €/MWh
<i>Subscripts and superscripts</i>	
0	Reference state
add	Additional
comp	Compressor
grid	Electric grid
m	Membrane
max	Maximum
min	Minimum
total	Power after installation of extra CAE stacks
ref	Reference
req	Required
stacks	Electrolysis stacks
transform	Transformer

References

1. Kondziella, H.; Bruckner, T. Flexibility requirements of renewable energy based electricity systems—A review of research results and methodologies. *Renew. Sustain. Energy Rev.* **2016**, *53*, 10–22. [[CrossRef](#)]
2. Torriti, J. *Peak Energy Demand and Demand Side Response*; Volume I: Fundamentals; Routledge: New York, NY, USA, 2016.
3. Electric Power Research Institute (EPRI). *Demand Side Management Glossary*; TR-101158 Project 1940-25 Final Report; McGraw-Hill Co.: Palo Alto, CA, USA, 1992.
4. U.S. Department of Energy. *Benefits of Demand Response in Electricity Markets and Recommendations for Achieving Them*; Report to the United States Congress: Washington, DC, USA, 2006.

5. Electric Power Research Institute (EPRI). New Principles for Demand Response Planning. In Proceedings of the 2013 IEEE Power & Energy Society General Meeting, Palo Alto, CA, USA, 21–25 July 2013.
6. North American Electric Reliability Corporation (NERC). *Demand Response Availability Data System (DADS): Phase I & II*; Final Report; Department of Civil and Environmental Engineering, University of South Florida: Tampa, FL, USA, 2011.
7. Paterakis, N.G.; Erdinç, O.; Catalão, J.P. An overview of Demand Response: Key-elements and international experience. *Renew. Sustain. Energy Rev.* **2017**, *69*, 871–891. [[CrossRef](#)]
8. Babu, C.A.; Ashok, S. Peak Load Management in Electrolytic Process Industries. *IEEE Trans. Power Syst.* **2008**, *23*, 399–405. [[CrossRef](#)]
9. Otashu, J.I.; Seo, K.; Baldea, M. Cooperative optimal power flow with flexible chemical process loads. *AIChE J.* **2021**, *67*, e17159. [[CrossRef](#)]
10. Ausfelder, F.; Seitz, A.; von Roon, S. Flexibilitätsoptionen in der Grundstoffindustrie. In *Bericht des AP V.6 Flexibilitätsoptionen und Perspektiven in der Grundstoffindustrie im Kopernikus-Projekt SynErgie*; Dechema: Frankfurt am Main, Germany, 2018. (In German)
11. Schimmel, M.; Achtelik, C.; Rhiemeier, J.M. Energiewende in der Industrie—Potenziale und Wechselwirkungen mit dem Energiesektor. In *Abschlussbericht zum Arbeitspaket 1: BMWi: I C 4 80 14 38/42*; Projekt-Nr. 42/17; Navigant: Berlin, Germany, 2019. (In German)
12. Arnold, K.; Janßen, T.; Echternacht, L.; Höller, S.; Voss, T.; Perrey, K. *Flexibilisation of Industries Enables Sustainable Energy Systems*; Report, Wuppertal Institute: Wuppertal, Germany, 2016.
13. Hoffmann, C.; Hübner, J.; Klaucke, F.; Milojević, N.; Müller, R.; Neumann, M.; Weigert, J.; Esche, E.; Hofmann, M.; Repke, J.U.; et al. Assessing the realizable flexibility potential of electrochemical processes. *Ind. Eng. Chem. Res.* **2021**, *60*, 13637–13660. [[CrossRef](#)]
14. Otashu, J.I.; Baldea, M. Demand response-oriented dynamic modeling and operational optimization of membrane-based chlor-alkali plants. *Comput. Chem. Eng.* **2019**, *121*, 396–408. [[CrossRef](#)]
15. Wang, X.; Teichgräber, H.; Palazoglu, A.; El-Farra, N.H. An economic receding horizon optimization approach for energy management in the chlor-alkali process with hybrid renewable energy generation. *J. Process Contr.* **2014**, *24*, 1318–1327. [[CrossRef](#)]
16. Chen, S.; Kumar, A.; Wong, W.C.; Chiu, M.S.; Wang, X. Hydrogen value chain and fuel cells within hybrid renewable energy systems: Advanced operation and control strategies. *Appl. Energy* **2019**, *233–234*, 321–337. [[CrossRef](#)]
17. Baetens, J.; Kooning, J.; Eetvelde, G.V.; Vandeveld, L. A Two-Stage Stochastic Optimisation Methodology for the Operation of a Chlor-Alkali Electrolyser under Variable DAM and FCR Market Prices. *Energies* **2020**, *13*, 5675. [[CrossRef](#)]
18. Teichgräber, H.; Brandt, A.R. Optimal design of an electricity-intensive industrial facility subject to electricity price uncertainty: Stochastic optimization and scenario reduction. *Chem. Eng. Res. Des.* **2020**, *163*, 204–216. [[CrossRef](#)]
19. Richstein, J.C.; Hosseinioun, S.S. Industrial demand response: How network tariffs and regulation (do not) impact flexibility provision in electricity markets and reserves. *Appl. Energy* **2020**, *278*, 115431. [[CrossRef](#)]
20. Klaucke, F.; Hoffmann, C.; Hofmann, M.; Tsatsaronis, G. Impact of the chlorine value chain on the demand response potential of the chloralkali process. *Appl. Energy* **2020**, *276*, 115366. [[CrossRef](#)]
21. Hofmann, M.; Müller, R.; Christidis, A.; Fischer, P.; Klauke, F.; Vomberg, S.; Tsatsaronis, G. Flexible and economical operation of chlor-alkali process with subsequent polyvinyl chloride production. *AIChE J.* **2022**, *68*, e17480. [[CrossRef](#)]
22. Geres, R.; Kohn, A.; Lenz, S.; Ausfelder, F.; Bazzanella, A.; Möller, A. *Roadmap Chemie 2050*; Report prepared by Dechema and FutureCamp for VCI; Munich, Germany, 2019. Available online: <https://geomodeling.njnu.edu.cn/modelItem/eaf8a0d7-afd8-48c0-bcd9-6d6ed8d169ed> (accessed on 20 March 2022). (In German)
23. Bruns, B.; Herrmann, F.; Polyakova, M.; Grünewald, M.; Riese, J. A systematic approach to define flexibility in chemical engineering. *J. Adv. Manuf. Process.* **2020**, *2*, e10063. [[CrossRef](#)]
24. Lahrsen, I.M.; Hofmann, M.; Müller, R. Models for the analysis of the flexible and economical operation of chlor-alkali process with subsequent epichlorohydrin production. *AIChE J.* **2022**, *68*, e17480. [[CrossRef](#)]
25. Hirth, L. *The European Electricity Market Model EMMA*; Model Documentation, Version 2017-07-12; Pergamon Press Ltd.: London, UK, 2017.
26. Kopiske, J.; Spieker, S.; Tsatsaronis, G. Value of power plant flexibility in power systems with high shares of variable renewables: A scenario outlook for Germany 2035. *Energy* **2017**, *137*, 823–833. [[CrossRef](#)]
27. Klein, S.A. *EES—Engineering Equation Solver, F-Chart Software*, Version 10.836; 2020. Available online: https://link.springer.com/chapter/10.1007/978-1-4613-0215-5_8 (accessed on 20 March 2022).
28. GAMS Development Corporation. *General Algebraic Modeling System (GAMS), Release 32.1.0*; Bantam Books, Inc.: New York, NY, USA, 2020.
29. GAMS Development Corporation. *CPLEX*; Version 12; Bantam Books, Inc.: New York, NY, USA, 2020.
30. Condon, M. Chemical Profile: Europe Epichlorohydrin. 2018. Available online: https://m.chemicalbook.com/ChemicalProductProperty_EN_CB8381781.htm (accessed on 20 March 2022).
31. Peters, M.; Ahrens, A. *Auswirkungen des REACH-Verfahrens auf die Herstellung von Epichlorhydrin Sowie die Anwendung Seiner Folgeprodukte als Kleber in der Automobilindustrie*; Research report; Niedersächsisches Umweltministerium: Hannover, Germany, 2006. (In German)
32. Euro Chlor. Chlor-alkali Industry Review 2018/2019. 2019. Available online: <https://www.chlorineindustryreview.com/> (accessed on 20 March 2022).

33. Schmittinger, P. *Chlorine: Principles and Industrial Practice*; Wiley-VCH: Weinheim, Germany, 2000. ISBN 9783527613380. [CrossRef]
34. O'Brien, T.F.; Bommaraju, T.V.; Hine, F. Overview of the Chlor-Alkali Industry. In *Handbook of Chlor-Alkali Technology*; Springer: Boston, MA, USA, 2005; pp. 37–74. [CrossRef]
35. Federal Institute for Occupational Safety and Health. *Ortsfeste Druckanlagen für Gase*; TRGS 746; Springer: Berlin/Heidelberg, Germany, 2016. (In German)
36. Gerrath, C. Recent Developments in Chlorine Processing. In Proceedings of the 55th Munich Technology Security Conference, Munich, Germany, 18–20 February 1999.
37. Krähling, L.; Krey, J.; Jakobson, G.; Grolig, J.; Miksche, L. Allyl Compounds. In *Ullmann's Encyclopedia of Industrial Chemistry*; Wiley-VCH: Weinheim, Germany, 2012; pp. 447–469. [CrossRef]
38. Johnson, G.F. Production of dichlorohydrin from allyl chloride. U.S. Patent 2,714,123a, 26 July 1955.
39. Liu, G.Y.T.; Richey, W.F.; Betso, J.E. Chlorohydrins. In *Ullmann's Encyclopedia of Industrial Chemistry*; Wiley-VCH: Weinheim, Germany, 2000. [CrossRef]
40. Kneupper, C.D.; Basile, P.S.; Noormann, S. Process and Apparatus for Producing and Purifying Epichlorohydrins. U.S. Patent 8,298,500, 30 December 2012.
41. Brée, L.C.; Perrey, K.; Bulan, A.; Mitsos, A. Demand side management and operational mode switching in chlorine production. *AIChE J.* **2019**, *65*, e16352. [CrossRef]
42. *Klimaschutzprogramm 2030 der Bundesregierung zur Umsetzung des Klimaschutzplans 2050*; Drucksache 19/13900; Federal Government: Stuttgart, Germany, 2019. (In German)
43. Ruhnau, O.; Bucksteeg, M.; Ritter, D.; Schmitz, R.; Böttger, D.; Koch, M.; Pöstges, A.; Wiedmann, M.; Hirth, L. *Why Electricity Market Models Yield Different Results: Carbon Pricing in a Model-Comparison Experiment*; Working Paper; Kiel: Hamburg, Germany, 2021.
44. Marktdaten. Dataset, Bundesnetzagentur. 2017–2019. Available online: https://www.researchgate.net/publication/220174356_Marktwirtschaftlicher_Datenschutz (accessed on 20 March 2022).
45. Internetplattform zur Vergabe von Regelleistung. Dataset, Regelleistung.net. 2017–2019. Available online: <https://www.vde-verlag.de/proceedings-en/453336006.html> (accessed on 20 March 2022).